AIAA 95-2430

Pulsed Instabilities in Combustion Chambers

V. S. Burnley, G. Swenson, and F. E. C. Culick
California Institute of Technology
Pasadena, CA

31st AIAA/ASME/SAE/ASEE
Joint Propulsion Conference and Exhibit
July 10-12, 1995/San Diego, CA

PULSED INSTABILITIES IN COMBUSTION CHAMBERS

V. Burnley*, G. Swenson†, and F.E.C. Culick‡
California Institute of Technology, Pasadena, California 91125

Abstract

A pulsed or "triggered" instability occurs when pressure oscillations develop in a linearly stable combustion system after being subjected to a sufficiently large disturbance. Such true nonlinear instabilities usually occur as subcritical bifurcations in dynamical systems theory. Understanding which nonlinear processes can lead to subcritical bifurcations is the focus of this work. Earlier work with the approximate analysis used here has shown convincingly that nonlinear acoustics alone does not contain the phenomenon of pulsed instabilities; evidently some other nonlinear contribution must also be included. An extensive experimental and numerical investigation conducted by Baum and Levine strongly suggests that nonlinear combustion is required. Using models of pressure and velocity coupling, the current work studies the effect of nonlinear combustion on the behavior of the system.

1 Introduction

Combustion instabilities were discovered as a serious problem in propulsion systems more than four decades ago. Since their discovery, two main types of instabilities have been observed in practice: spontaneous instabilities and pulsed instabilities. Spontaneous instabilities occur in combustion systems which are linearly unstable so that any disturbance initially grows exponentially in time. Under the influence of nonlinear processes, the oscillations may reach a limiting amplitude. Pulsed instabilities, also known as "triggering," occur in systems which are stable to small perturbations but are unstable to larger disturbances.

Methods of analyzing spontaneous oscillations are now highly developed,[1,2] though it cannot be claimed that predictions and interpretations of observed behavior can be accomplished with wholly satisfying accuracy. However, experience has shown that the errors and uncertainties are, almost certainly, due in all cases to imperfect information required to produce quantitative results. The most significant uncertainties are associated with the response of combustion to unsteady motions, but none of the contributing processes are well understood.

Pulsed instabilities have received less attention, and methods are thus less advanced. This seems to be partly due to difficulties in analysis, and partly to less pressing practical concern compared with the widespread need for coping with problems of spontaneous instabilities early in the development of propulsion systems. The most extensive investigation of pulsed oscillations, both experimentally and theoretically, was conducted by the Air Force Rocket Propulsion Laboratory beginning in the mid-1970s lasting through 1988.[3] As part of the effort to understand experimental observations, Baum and Levine used numerical methods to solve partial differential equations (PDEs) approximating the experiments. Nonlinear combustion was modeled using a nonlinear combustion response based on the idea of velocity coupling – the unsteady equivalent of erosive burning.

There are certain drawbacks to using a purely numerical method to interpret data. It is often difficult, for example, to produce general trends useful in the design process. Also, numerical methods do not readily allow one to determine the relative influence

*Graduate Student; Student Member AIAA
†Graduate Student
‡Professor of Mechanical Engineering and Jet Propulsion; Fellow AIAA

and importance of the various nonlinear processes. Nonetheless, the results of Baum and Levine showed convincingly that nonlinear combustion is an important process in triggering to a stable limit cycle.

For the reasons cited above, an approximate analysis is better suited for the purposes of this work. The approximate analysis used here was introduced by Zinn,[4–6] and independently, by Culick.[7,8] It is based on application of spatial averaging in the form of Galerkin's method, which has proven to be a very useful technique in the study of combustion instabilities.

Over the past twenty years, this approximate analysis has been used extensively to study the effects of nonlinear processes on combustion instabilities. Although it has not been proven explicitly, calculations for a wide range of special cases have shown that nonlinear gasdynamics alone does not contain pulsed instabilities.[9–12] The reason seems to be that nonlinear gasdynamic coupling causes transfer of energy among acoustic modes in a special way. Any possible transfer of internal thermodynamic energy to the energy of a pulse takes place at a rate insufficient to compensate the dissipation of energy causing the acoustic system to be linearly stable.

Other investigations have studied acoustics-mean flow interactions as a possible mechanism of triggering. While the mean flow offers a significant energy source which could possibly sustain such oscillations, the investigation by Yang et al.[10] did not reveal any conditions under which triggering will occur.

Nonlinear combustion processes have also been treated in the context of the approximate analysis. Gadiot and Gany[13] reported triggering when nonlinear pressure coupling was included. However, the validity of the results are questionable due to the high amplitudes of the oscillations. In addition, limited results of triggering have been obtained by Kim[14] and Greene[15] using ad hoc velocity coupled models along with the additional approximations of time-averaging and truncation to two modes.

More recently, pulsed instabilities were treated in the companion paper of this work.[16] Using two ad hoc models of velocity coupling, dynamical systems theory was used to study the effects of nonlinear combustion and gasdynamics. Results were obtained for up to six modes, both with and without the approximation of time-averaging.

The current study is an extension of that article. The present investigation also uses dynamical systems theory to study nonlinear pressure coupling and to extend the nonlinear velocity coupled models to account for threshold velocity effects. Discrepancies in results obtained with and without time-averaging are also addressed.

2 Formulation of the Approximate Analysis

The development of the approximate analysis has been covered in many works beginning in 1976[8] and most recently in the companion article of this work.[16] As with any analysis of the flow in a liquid or solid rocket, the development must begin with the conservation equations for two-phase flow. A wave equation for the pressure is then derived for a medium having the mass-averaged properties of the mixture of gas and particulate matter.[1] As an approximation to the unsteady pressure and velocity fields, we will use the classical acoustic modes of the chamber ψ_m as an orthogonal basis:

$$p'(\boldsymbol{r},t) = \bar{p}\sum_{m=1}^{\infty}\eta_m(t)\psi_m(\boldsymbol{r}) \tag{1}$$

$$\boldsymbol{u}'(\boldsymbol{r},t) = \sum_{m=1}^{\infty}\frac{\dot{\eta}_m(t)}{\gamma k_m^2}\nabla\psi_m(\boldsymbol{r}) \tag{2}$$

The time-dependent amplitudes $\eta_m(t)$ will eventually be the variables to be determined. Substitution of these approximations in the wave equation followed by spatial averaging transforms the problem from a system of PDEs to a system of ODEs, a notable simplification.

$$\frac{d^2\eta_n}{dt^2} + \omega_n^2\eta_n = F_n \tag{3}$$

where $\omega_n = ak_n$ and

$$F_n = -\frac{a^2}{\bar{p}E_n^2}\left\{\int\psi_n h dV + \oint\psi_n f dS\right\} \tag{4}$$

Generally, F_n will depend both linearly and nonlinearly on the pressure and velocity fluctuations. If

we deal only with acoustic motions, then it is appropriate to use Eqs. (1) and (2) to evaluate F_n, thereby introducing η_n and $\dot{\eta}_n$ in the right hand side of Eq. (3). Further considerations are necessary to treat more general unsteady motions, as we shall discuss in Sec. 3.

For the numerical results discussed in Sec. 4, we shall treat only longitudinal modes normally excited in straight chambers having uniform cross-section. Neglecting nonlinear contributions other than gasdynamics and combustion, we obtain the following set of coupled nonlinear oscillators.[9]

$$\ddot{\eta}_n + \omega_n^2 \eta_n = 2\alpha_n \dot{\eta}_n + 2\omega_n \theta_n \eta_n - \sum_{i=1}^{n-1} (C_{ni}^{(1)} \dot{\eta}_i \dot{\eta}_{n-i} + D_{ni}^{(1)} \eta_i \eta_{n-i}) - \sum_{i=1}^{\infty} (C_{ni}^{(2)} \dot{\eta}_i \dot{\eta}_{n+i} + D_{ni}^{(2)} \eta_i \eta_{n+i}) + (F_n)_{\text{comb}}^{\text{NL}} \quad (5)$$

where $(F_n)_{\text{comb}}^{\text{NL}}$ will be replaced by one of the nonlinear combustion models which will be developed in the next section and

$$C_{ni}^{(1)} = \frac{-1}{2\gamma i(n-i)}[n^2 + i(n-i)(\gamma-1)]$$

$$C_{ni}^{(2)} = \frac{1}{\gamma i(n+i)}[n^2 - i(n+i)(\gamma-1)]$$

$$D_{ni}^{(1)} = \frac{(\gamma-1)\omega_1^2}{4\gamma}[n^2 - 2i(n-i)]$$

$$D_{ni}^{(2)} = \frac{(\gamma-1)\omega_1^2}{2\gamma}[n^2 + 2i(n+i)]$$

Many previous investigations using the approximate analysis have also used the method of time-averaging. The idea is that in many applications, the oscillations have slowly varying amplitudes and phases: only small fractional changes in one period of the lowest mode. It is then reasonable to write (without approximation at this point),

$$\eta_n(t) = r_n(t)\sin[\omega_n t + \phi_n(t)] = A_n(t)\sin\omega_n t + B_n(t)\cos\omega_n t \quad (6)$$

where A_n and B_n are assumed to be slowly varying in time. Substituting this expression in Eq. (3) followed by averaging over one period of the fundamental mode yields

$$\frac{dA_n}{dt} = \frac{1}{\omega_n \tau_1}\int_t^{t+\tau_1} F_n \cos\omega_n t' dt' \quad (7a)$$

$$\frac{dB_n}{dt} = -\frac{1}{\omega_n \tau_1}\int_t^{t+\tau_1} F_n \sin\omega_n t' dt' \quad (7b)$$

When the integrals are carried out, the A_n and B_n in F_n are assumed constant since they vary little over the time of integration, τ_1. The companion article calculated solutions using the method of time-averaging in order to determine the effect of this approximation.

3 Modeling Nonlinear Combustion Response of a Solid Propellant

Analysis of unsteady burning has been directed largely to investigating the response of burning to fluctuations of the flow field, in order to satisfy the needs for predicting linear stability. Most of the results were obtained early in the development of the subject; see Culick[17] for a review of calculations of the response function.

Motivated by observations suggesting that the response of a burning solid likely depends on the scouring effect of flow velocity parallel to the surface, McClure and his colleagues[18,19] treated the corresponding phenomenon for unsteady motions. The idea is that changes in the burning rate of a solid may be dependent on changes of the magnitude but not the direction of the flow past the surface. The simplest possible cause of such behavior is associated with convective heat transfer. Whatever its true physical origin, this sort of nonlinear behavior is commonly called "velocity coupling." In the first instance, including this effect in analysis of the unsteady burning rate introduces essentially a kinematical nonlinearity. Without a thorough analysis of the entire burning process, it is not possible to state unequivocally the form that the nonlinearity should take.

For the purposes here, the precise formula for nonlinear unsteady combustion is unimportant. We intend primarily to determine the effect of nonlinear

combustion on the behavior of the nonlinear system. Two models are used in this investigation; one representing nonlinear pressure coupling, and one representing velocity coupling with a threshold velocity. The pressure coupled model is derived by extending the derivation of a linear response function to include second-order terms. The threshold velocity model is a modification of the velocity coupled model proposed by Greene.[15] This model was also used in the companion article.

In order to be used in the present analysis, any model of unsteady combustion must be put in such a form as to fit into the appropriate terms in the forcing function given by Eq. (4). For gasdynamics up to second-order, the right hand side of Eq. (4) can be written:

$$-\frac{\bar{p}E_n^2}{a^2}F_n = \left\{\bar{\rho}\int(\bar{\boldsymbol{u}}\cdot\nabla\boldsymbol{u}' + \boldsymbol{u}'\cdot\nabla\bar{\boldsymbol{u}})\cdot\nabla\psi_n dV + \frac{1}{a^2}\frac{\partial}{\partial t}\int(\gamma p'\nabla\cdot\bar{\boldsymbol{u}} + \bar{\boldsymbol{u}}\cdot\nabla p')\psi_n dV\right\}$$

linear gasdynamics

$$+\left\{\bar{\rho}\int\left[\boldsymbol{u}'\cdot\nabla\boldsymbol{u}' + \frac{\rho'}{\bar{\rho}}\frac{\partial\boldsymbol{u}'}{\partial t}\right]\cdot\nabla\psi_n dV + \frac{1}{a^2}\frac{\partial}{\partial t}\int(\gamma p'\nabla\cdot\boldsymbol{u}' + \boldsymbol{u}'\cdot\nabla p')\psi_n dV\right\} \quad (8)$$

nonlinear gasdynamics

$$+\oint\bar{\rho}\frac{\partial\boldsymbol{u}'}{\partial t}\cdot\hat{\boldsymbol{n}}\psi_n dS - \int\left[\frac{1}{a^2}\frac{\partial\mathcal{P}'}{\partial t}\psi_n + \mathcal{F}'\cdot\nabla\psi_n\right]dV$$

linear and nonlinear surface processes — other contributions

All terms in the first two pairs of brackets labeled linear and nonlinear gasdynamics will be computed using the zeroth-order approximations (1) and (2) for the pressure and velocity as described in Sec. 2. Those terms labeled "other contributions", containing for example, interactions between the gas and condensed phase, will be ignored here.

As a means of accommodating nonlinear combustion of solid propellants, we are concerned in this section with the remaining terms arising from unsteady processes on the boundary of the chamber*. Part of this contribution is due to the exhaust nozzle and will be absorbed in the linear attenuation. For the nonlinear combustion, the term labeled "surface processes" nearly equals the time derivative of the second-order fluctuation of mass flux inward. The mass flux at the surface is defined as $\dot{m} = \rho u$ so that the fluctuating part becomes

$$\begin{aligned}\dot{m}' &= \dot{m} - \bar{\dot{m}}\\ &= (\bar{\rho}+\rho')(\bar{u}+u') - \bar{\rho}\bar{u}\\ &= \bar{\rho}u' + \rho'(\bar{u}+u')\end{aligned}$$

Taking the time derivative and rearranging terms, we obtain a form which can be substituted into Eq. (8).

$$\bar{\rho}\frac{\partial\boldsymbol{u}'}{\partial t}\cdot\hat{\boldsymbol{n}} = \frac{\partial\dot{m}'}{\partial t}\cdot\hat{\boldsymbol{n}} - \rho'\frac{\partial\boldsymbol{u}'}{\partial t}\cdot\hat{\boldsymbol{n}} - \frac{\partial\rho'}{\partial t}(\bar{\boldsymbol{u}}+\boldsymbol{u}')\cdot\hat{\boldsymbol{n}} \quad (9)$$

It happens that analysis and modeling of unsteady combustion leads to results for mass fluctuation but, as shown by Eq. (8), the gasdynamics problem within the chamber requires the unsteady velocity as the boundary condition. Thus we can include contributions from nonlinear combustion by use of Eq. (9). Substitution of Eq. (9) into the surface process term of Eq. (8) gives

$$-\frac{\bar{p}E_n^2}{a^2}(F_n)_{\text{comb}} = \oint\frac{\partial\dot{m}'}{\partial t}\cdot\hat{\boldsymbol{n}}\psi_n dS - \oint\rho'\frac{\partial\boldsymbol{u}'}{\partial t}\cdot\hat{\boldsymbol{n}}\psi_n dS - \oint\frac{\partial\rho'}{\partial t}(\bar{\boldsymbol{u}}+\boldsymbol{u}')\cdot\hat{\boldsymbol{n}}\psi_n dS \quad (10)$$

To evaluate the last two integrals, the linear approximation for $\boldsymbol{u}'$ expressed in terms of the admittance function A_b will be used:[1]

$$-\boldsymbol{u}'\cdot\hat{\boldsymbol{n}} = aA_b\frac{p'}{\gamma\bar{p}} \quad (11)$$

*It should be noted that the approximate analysis can also accommodate nonlinear combustion processes of liquid propellants through the terms labeled "other contributions."

Using this approximation along with the isentropic assumption, $\rho' = \bar{\rho}p'/\gamma\bar{p}$, yields

$$-\frac{\bar{p}E_n^2}{a^2}(F_n)_{\text{comb}} = -\oint \frac{\partial \dot{m}'}{\partial t}\psi_n dS + \bar{\rho}\oint\left(\bar{u}_b + 2aA_b\frac{p'}{\gamma\bar{p}}\right)\frac{\partial}{\partial t}\left(\frac{p'}{\gamma\bar{p}}\right)\psi_n dS \quad (12)$$

where we have defined $\bar{u}_b = -\bar{\boldsymbol{u}}\cdot\hat{\boldsymbol{n}}$ and $\dot{m}' = -\dot{\boldsymbol{m}}'\cdot\hat{\boldsymbol{n}}$ to simplify the equations.

3.1 Second-Order Pressure Coupling

The linear response of a solid propellant to pressure fluctuations at the flame has been treated in many analyses, usually leading to the same two parameter expression as found by Denison and Baum.[17,20] The form of the two parameters depend on the models chosen for the solid and gas phases. Here, we will derive the nonlinear response by retaining terms to second-order in fluctuations using the following models for the solid and gas phase: 1) the solid is assumed to be homogeneous and nonreactive with constant properties, 2) combustion is assumed to be uniformly distributed with combustion beginning immediately at the solid-gas interface, 3) combustion responds quasi-statically to fluctuations in pressure only. The linear response for this special case has been previously treated by Culick,[21] so many of the details will not be covered here.

3.1.1 The Solid Phase and Solid-Gas Interface

We begin with the energy balance at the solid-gas interface.

$$\left(k_g\frac{dT}{dx}\right)'_{s+} = \left(k_p\frac{dT}{dx}\right)'_{s-} + (c_p - c)\bar{\dot{m}}_s T'_s + Q_s\dot{m}'_s + (c_p - c)\dot{m}'_s T'_s \quad (13)$$

where the subscript s denotes the value at the solid-gas interface. Q_s is the heat released at the surface, while c_p and c are the specific heats of the gas and solid, respectively. This will be the main equation into which the solutions from the solid and gas phases will be substituted. Under the assumptions listed above, solution for the solid phase yields the fluctuation of heat transfer from the interface to the solid.

$$\left(k_p\frac{dT}{dx}\right)'_{s-} = \bar{\dot{m}}_s c\bar{T}_s\left[\lambda\frac{T'_s}{\bar{T}_s} + \frac{1 - \frac{T_c}{\bar{T}_s}}{\lambda}\frac{\dot{m}'_s}{\bar{\dot{m}}_s}\right] \quad (14)$$

λ is a complex function of frequency found by solving the equation $\lambda(\lambda - 1) = i\kappa_p\omega/\bar{r}_b^2$; T_c is the temperature of the cold propellant. To complete the analysis of the solid-gas interface, an assumption regarding the rate of conversion of solid to gas must be made. As is common practice, an Arrhenius Law will be used for pyrolysis at the surface.

$$m_s = B_s T_s^{\beta_1} e^{-E_s/R_0T_s} \quad (15)$$

To second-order in fluctuations, the mass flux is given by

$$\frac{\dot{m}'_s}{\bar{\dot{m}}_s} = (\beta_1 + \bar{E})\frac{T'_s}{\bar{T}_s} + \left[\frac{\beta_1(\beta_1 - 1)}{2} + \beta_1\bar{E} + \left(\frac{\bar{E}^2}{2} - \bar{E}\right)\right]\left(\frac{T'_s}{\bar{T}_s}\right)^2 \quad (16)$$

where

$$\bar{E} \equiv \frac{E_s}{R_0\bar{T}_s}$$

Combining Eqs. (13), (14), and (16) leads to an equation relating the surface temperature fluctuations to the heat transfer from the gas to the solid-gas interface.

$$\left(k_g\frac{dT}{dx}\right)'_{s+} = \bar{\dot{m}}_s c\bar{T}_s\left[C_1\frac{T'_s}{\bar{T}_s} + C_2\left(\frac{T'_s}{\bar{T}_s}\right)^2\right] \quad (17)$$

where

$$C_1 = \lambda + \frac{A}{\lambda} + \left(\frac{c_p}{c} - 1\right) - \frac{Q_s(\beta_1 + \bar{E})}{c\bar{T}_s}$$

$$C_2 = \left(\frac{c_p}{c} - 1\right)(\beta_1 + \bar{E}) + \left(\frac{1 - \frac{T_c}{\bar{T}_s}}{\lambda} - \frac{Q_s}{c\bar{T}_s}\right) \times \left[\frac{\beta_1(\beta_1 - 1)}{2} + \beta_1\bar{E} + \left(\frac{\bar{E}^2}{2} - \bar{E}\right)\right]$$

$$A = (\beta_1 + \bar{E})\left(1 - \frac{T_c}{\bar{T}_s}\right)$$

3.1.2 The Gas Phase

The solution for the gas phase gives another formula for the fluctuation of heat transfer to the solid.

$$\left(k_g \frac{dT}{dx}\right)'_{s+} = \bar{\dot{m}} c_p \bar{T}_s \Lambda^2 \left[\frac{w'}{\bar{w}} - \frac{\dot{m}'_s}{\bar{\dot{m}}_s} - \frac{w'}{\bar{w}}\frac{\dot{m}'_s}{\bar{\dot{m}}_s} + \left(\frac{\dot{m}'_s}{\bar{\dot{m}}_s}\right)^2\right] \quad (18)$$

where

$$\Lambda^2 = \frac{Q_f k_g \bar{w}}{\bar{\dot{m}}^2 c_p^2 \bar{T}_s}$$

This expression introduces an additional variable, the reaction rate w. Thus, we need another relation between the pressure and the reaction rate to complete the analysis. We assume that the reaction rate can be expressed as a function of pressure only and that the linear burning rate may be approximated by $\dot{m} = ap^n$. This leads to the following second-order equation relating the reaction rate and pressure.

$$\frac{c_p}{c}\left(\frac{\Lambda^2}{1-\frac{T_c}{T_s}}\right)\frac{w'}{\bar{w}} = W_1 \frac{p'}{\bar{p}} + W_2 \left(\frac{p'}{\bar{p}}\right)^2 \quad (19)$$

where

$$W_1 = 2n(1-H) + \frac{c_p}{c}\frac{n}{A}$$
$$W_2 = (2n^2 - n)(1-H) + \frac{2n^2}{A}\frac{c_p}{c} + \frac{c_p}{c}\frac{n(n-A)}{2A^2}$$

Substitution of Eq. (19) into Eq. (18) yields

$$\left(k_g \frac{dT}{dx}\right)'_{s+} = \frac{\bar{\dot{m}} c \bar{T}_s}{(\beta_1 + \bar{E})}\left[W_1 A \frac{p'}{\bar{p}} + W_2 A \left(\frac{p'}{\bar{p}}\right)^2 - \frac{c_p}{c}(\beta_1 + \bar{E})\Lambda^2 \frac{\dot{m}'_s}{\bar{\dot{m}}_s} - W_1 A \frac{p'}{\bar{p}}\frac{\dot{m}'_s}{\bar{\dot{m}}_s} + \frac{c_p}{c}(\beta_1 + \bar{E})\Lambda^2 \left(\frac{\dot{m}'_s}{\bar{\dot{m}}_s}\right)^2\right] \quad (20)$$

Finally, equating Eqs. (20) and (17) followed by substitution for T'_s from Eq. (16) leads to the nonlinear response function. In the linear limit, the response function can be written in the two parameter form of Denison and Baum.[20]

$$R_b^{\text{linear}} = \frac{\dot{m}'/\bar{\dot{m}}}{p'/\bar{p}} = \frac{nAB}{\lambda + \frac{A}{\lambda} - (1+A) + AB} \quad (21)$$

with

$$B = 2\left(1 - \frac{Q_s}{c(\bar{T}_s - T_c)}\right) + \frac{c_p}{c}\frac{1}{A} \quad (22)$$

Using this definition, the nonlinear response function is written as a function of the linear response function.

$$R_b^{\text{n.l.}} = R_b^{\text{linear}} + \left[\frac{W_2}{W_1} R_b^{\text{linear}} - \left(R_b^{\text{linear}}\right)^2 - \frac{D}{AW_1}\left(R_b^{\text{linear}}\right)^3\right]\left(\frac{p'}{\bar{p}}\right) \quad (23)$$

where

$$D = \left(\frac{c_p}{c} - 1\right)\left(1 - \frac{C_3}{C_4^2}\right) - \lambda\frac{C_3}{C_4^2} - \frac{c_p}{c}C_4\Lambda^2$$
$$C_3 = \frac{\beta_1(\beta_1 - 1)}{2} + \beta_1 \bar{E} + \left(\frac{\bar{E}^2}{2} - \bar{E}\right)$$
$$C_4 = \beta_1 + \bar{E}$$

The linear response function is a complex quantity in general. When used in calculations of time-dependent motions, an approximation to R_b^{linear} can be made for pure oscillations

$$[R_b^{(r)} + iR_b^{(i)}]e^{i\omega t} = \left[R_b^{(r)} + R_b^{(i)}\frac{1}{\omega}\frac{\partial}{\partial t}\right]e^{i\omega t} \quad (24)$$

Hence, to incorporate the linear response functions in the analysis, we may set

$$R_b^{\text{linear}} = R_b^{(r)} + R_b^{(i)}\frac{1}{\omega}\frac{\partial}{\partial t} \quad (25)$$

since to zero order, we have pure oscillatory motions. ω is taken to be ω_n in the n^{th} oscillator equation. It is assumed that the nonlinear response function can be handled in the same manner.

3.2 Threshold Velocity Model

In the companion work,[16] two ad hoc velocity coupled models were used to study the effects of nonlinear combustion on the solution to the coupled nonlinear equations. The first model was proposed by Baum and Levine.[3] In this model, the mass burning rate is modified by a function of velocity as follows:

$$\dot{m} = \dot{m}_{\rm pc}[1 + R_{\rm vc}F(\boldsymbol{u})] \tag{26}$$

where $\dot{m}_{\rm pc}$ is the mass flux due to linear pressure coupling only and $R_{\rm vc}$ is the velocity coupled response function. $F(\boldsymbol{u}) = |\boldsymbol{u}'|$ was chosen since the burn rate should depend on the magnitude but not the direction of the parallel flow. Any possible influences of the mean flow are ignored at the present time.

$$\dot{m} = \dot{m}_{\rm pc}[1 + R_{\rm vc}|\boldsymbol{u}'|] \tag{27}$$

The second model, suggested by Greene,[15] is a subset of Baum and Levine's model. In this model, the fluctuating part of the mass flux is assumed to depend only on the magnitude of the velocity at the surface.

$$\dot{m}' = \bar{\dot{m}}R_{\rm vc}|\boldsymbol{u}'| \tag{28}$$

Results for these two models have been reported in the companion article and will be discussed further in Sec. 4.2.

Threshold effects have been observed in experimental investigations of velocity coupling.[22] We will investigate the possible influences of such a threshold using a modified form of Greene's model. Instead of using a direct dependence on the magnitude of velocity, the following model will be used.

$$\dot{m}' = \bar{\dot{m}}R_{\rm vc}F(\boldsymbol{u}') \tag{29}$$

where $F(\boldsymbol{u})$ is shown in Fig. 1. This function introduces a dead zone in which the nonlinear contribution from combustion does not affect the system. When the amplitudes of oscillations become larger than the chosen threshold value u_t, the nonlinear effects are then felt.

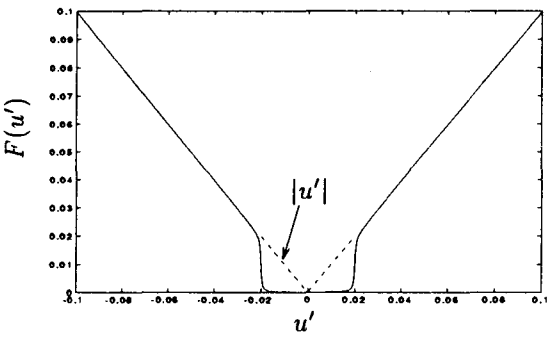

Figure 1: Threshold velocity function; $u_t = 0.02$

4 Discussion of Results

Dynamical systems theory was first applied to the study of nonlinear combustion instabilities by Jahnke and Culick.[23] As demonstrated by that work and by Culick et al.,[16] dynamical systems theory is indeed a very useful tool, allowing general trends to be obtained in a systematic manner.

As in the previous studies, we will use a continuation method to trace periodic solutions as a function of a free parameter of the system. Here the free parameter is chosen to be the linear growth rate of the first mode, α_1. The linear growth rates of all other modes are negative so that $\alpha_1 < 0$ denotes a linearly stable system. The results are presented as the maximum value of η_1 in the limit cycle as a function of α_1. For details on the continuation method, see Jahnke and Culick[23] and Doedel et al.[24,25]

4.1 Nonlinear Pressure Coupling

Even for small amplitude oscillations, the nonlinear response function can differ substantially from the linear response function as shown in Figs. 2 and 3 for $A = 6.0$ and $B = 0.55$. When $p'/\bar{p} = 0.01$, the second-order terms increase the magnitudes of both the real and imaginary parts of the response function substantially. Nonetheless, no triggering has been found for these parametric values, as well as other realistic values of A and B. The parameter space is large, so it is quite possible that this nonlinear model could lead to triggering for some values. So

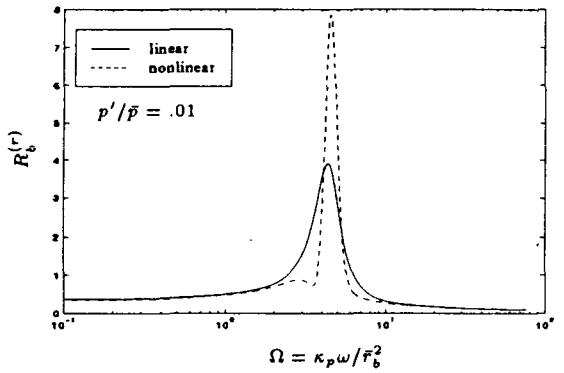

Figure 2: Real part of the linear and nonlinear propellant response functions vs. nondimensional frequency; $A = 6.0, B = 0.55, n = 0.3$

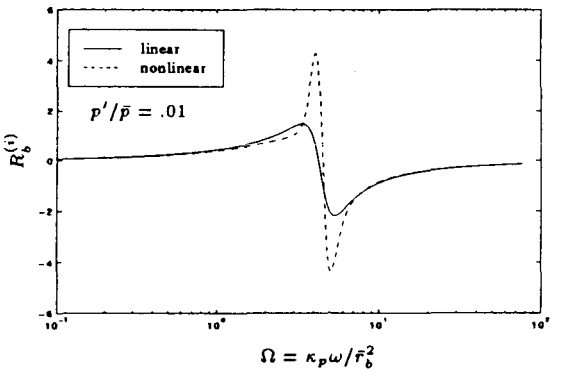

Figure 3: Imaginary part of the linear and nonlinear propellant response functions vs. nondimensional frequency; $A = 6.0, B = 0.55, n = 0.3$

far, however, the search has been unsuccessful.

For the case of nonlinear pressure coupling, it is important to know the linear stability boundary of the propellant response. Culick[17] reported the following stability criterion for the parameters of the linear response function.

$$A < (B+1)/(B-1)^2 \tag{30}$$

If this condition is not met, the propellant is intrinsically unstable and the values of A and B are not realistic.

Interesting enough, triggering to stable limit cycles was found for values of A and B outside this stability limit. The values given in Table 1 yield $A = 6.0$ and $B = 0.486$, which are located just outside the the stability boundary. As a result, the response functions, shown in Figs. 4 and 5 are quite different.

The results for truncation to two and four modes are displayed in Figs. 6 and 7. In both cases, a region of triggering was found. We have no explanation for this behavior at the present time. Although the values are unrealistic, this case may be useful if it helps gain a better understanding of the coupling between modes.

4.2 The Discrepancy between the Time-Averaged and Original Oscillator Equations

Results reported previously for velocity coupling, showed a substantial difference in the behavior predicted by the original oscillator equations and the time-averaged equations. The original oscillator equations produce a subcritical Hopf bifurcation at the origin with a very low amplitude unstable branch. The time-averaged results, however, show an α-shift, so that branching to periodic solutions occurs at a negative value of α_1. This bifurcation can be either subcritical or supercritical depending on other parameters of the system. Figures 8 and 9 show bifurcation diagrams for the original oscillator and the time-averaged equations, respectively.

After further consideration, it is now apparent that this discrepancy is the result of an approximation used when applying the continuation method to the original oscillator equations. Since the continuation method is based on the implicit function theorem, it is required that all functions be continuously differentiable. To meet this requirement, an approximation to $|u'|$ was used in the velocity coupled models. All plots reported in the companion paper utilized $|u'| \approx u' \frac{2}{\pi} \arctan(1000u')$. As Fig. 10 illustrates, the two functions are very different near $u' = 0$. Although this approximation was necessary,

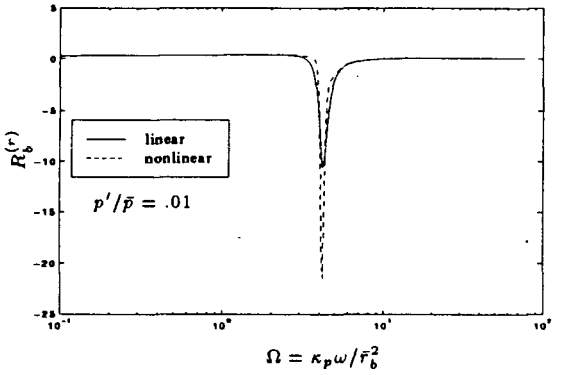

Figure 4: Real part of the linear and nonlinear propellant response functions vs. nondimensional frequency; $A = 6.0, B = 0.486, n = 0.3$

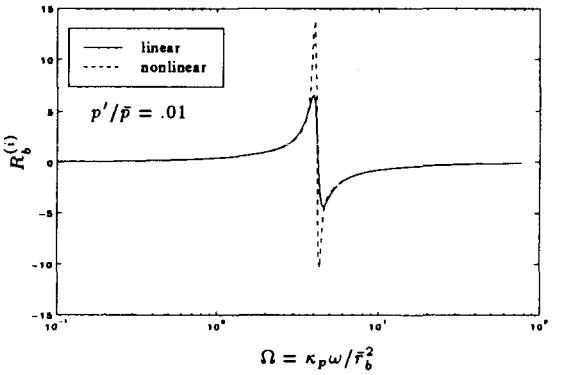

Figure 5: Imaginary part of the linear and nonlinear propellant response functions vs. nondimensional frequency; $A = 6.0, B = 0.486, n = 0.3$

it changed the nature of the equations by introducing an artificial threshold velocity. The threshold is very small, but it changes the behavior of the system from a shifted spontaneous oscillation to an apparent region of triggering. Therefore, the original oscillator equations should in fact produce results similar to those predicted by the time-averaged equations, i.e., a much smaller region of triggering or none at all.

This result suggests that a threshold velocity may be important in triggering. In the next section, we will study the possible effects of a larger threshold velocity.

4.3 Threshold Velocity Effects

The results obtained using the threshold velocity model do in fact lead to triggering as suggested by the above discussion. It is expected that since the nonlinear effects from combustion will not be felt until the threshold velocity is reached, at low amplitudes of oscillations, the path should be identical to the case of zero velocity coupling, i.e., a supercritical bifurcation at the origin. This is precisely the behavior shown in Fig. 11.

Once the threshold velocity is attained, nonlinear combustion quickly becomes important, and a fold in the path is produced. This unstable path follows a near horizontal path until other nonlinear effects

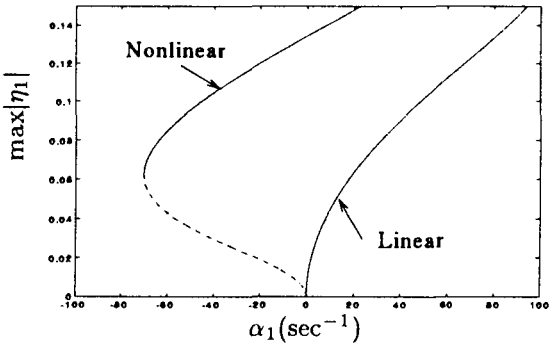

Figure 6: Maximum amplitude in limit cycle of first acoustic mode with linear and nonlinear pressure coupling; two modes, $A = 6.0$, $B = 0.486$

become strong enough to produce a second fold. It is also to be expected that the the amplitudes of oscillations will be smaller for this case than the zero threshold case due to the dead zone in the nonlinear response.

5 Concluding Remarks

Using an approximate analysis and the tools of dynamical systems theory, the present work has studied pulsed instabilities in combustion chambers. Since nonlinear combustion processes likely play an important role in this type of instability, two non-

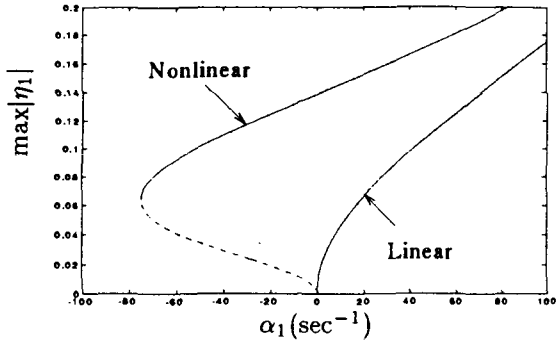

Figure 7: Maximum amplitude in limit cycle of first acoustic mode with linear and nonlinear pressure coupling; four modes, $A = 6.0$, $B = 0.486$

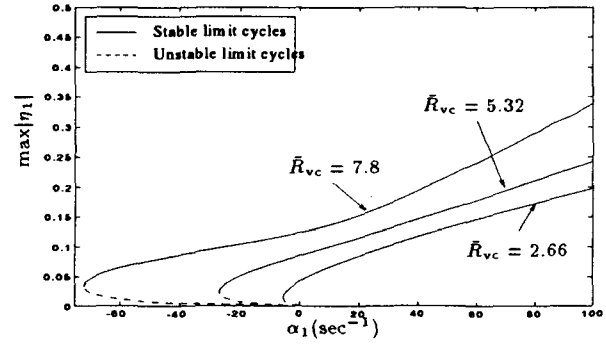

Figure 8: Maximum amplitude of first acoustic mode in limit cycle using Greene's model with the original oscillator equations and various values of $\bar{R}_{vc}$; four modes

linear combustion models were used in the analysis. The first model was a nonlinear pressure coupled model and was developed by extending the derivation of a linear response function to include second-order terms. This particular model did not exhibit triggering when realistic values of A and B were used, although a more thorough parameter search should be preformed. The second model extended Greene's velocity coupled model to study the effects of a threshold velocity. As expected, the threshold velocity model produced a large region of triggering.

Previous results showed a discrepancy between results obtained using the time-averaged equations

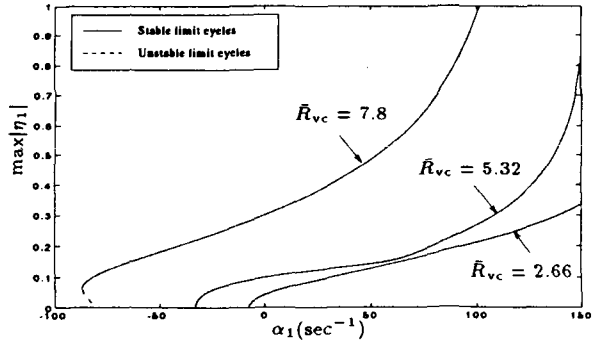

Figure 9: Maximum amplitude of first acoustic mode in limit cycle using Greene's model with the time-averaged equations and various values of $\bar{R}_{vc}$; four modes

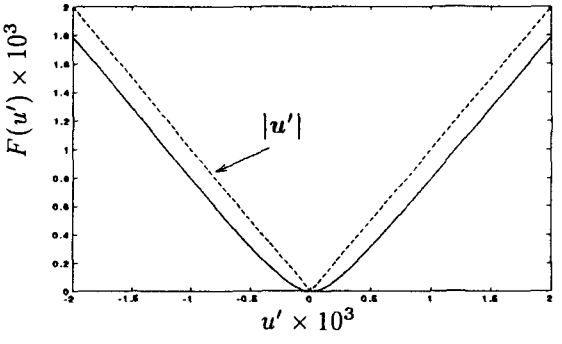

Figure 10: Approximation to $|u'|$ using the arctan function

and the original oscillator equations. The cause was determined to be an approximation used to make the original oscillator equations continuously differentiable, a necessary condition for use in the continuation method.

Acknowledgments

This work was partly supported by the Palace Knight Program of the U. S. Air Force, and partly by the California Institute of Technology, Pasadena, California.

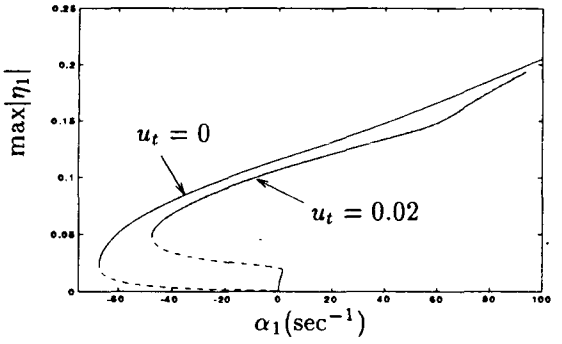

Figure 11: Maximum amplitude in limit cycle of first acoustic mode with and without a threshold velocity of 0.02; four modes; $\bar{R}_{vc} = 7.8$

References

[1] Culick, F. E. C. and Yang, V., "Prediction of the Stability of Unsteady Motions in Solid Propellant Rocket Motors", chapter 18 in *Nonsteady Burning and Combustion Stability of Solid Propellants*, Progress in Astronautics and Aeronautics, Vol. 143, 1992, p. 719.

[2] Nickerson, G. R., Culick, F. E. C., and Dang, L. G., "Standard Stability Prediction Method for Solid Rocket Motors, Axial Mode Computer Program, User's Manual", Software and Engineering Associates, Inc.; Air Force Rocket Propulsion Lab, Technical Report AFRPL-TR-83-017, Edwards AFB, CA, 1983.

[3] Baum, J. D., Levine, J. N., and Lovine, R. L., "Pulsed Instability in Rocket Motors; A Comparison Between Predictions and Experiments", *Journal of Propulsion and Power*, Vol. 4, No. 4, 1988, pp. 308–316.

[4] Zinn, B. T. and Powell, E. A., "Application of the Galerkin Method in the Solution of Combustion Instability Problems", *Proceedings of the 19th International Astronautical Congress*, Vol. 3, 1970, pp. 59–73.

[5] Zinn, B. T. and Lores, E. M., "Application of the Galerkin Method in the Solution of Nonlinear Axial Combustion Instability Problems in Liquid Rockets", *Combustion Science and Technology*, Vol. 4, No. 6, 1972, pp. 269–278.

[6] Lores, E. M. and Zinn, B. T., "Nonlinear Longitudinal Instability in Rocket Motors", *Combustion Science and Technology*, Vol. 7, No. 6, 1973, pp. 245–256.

[7] Culick, F. E. C., "Nonlinear Growth and Limiting Amplitude of Acoustic Oscillations in Combustion Chambers", *Combustion Science and Technology*, Vol. 3, No. 1, 1971, pp. 1–16.

[8] Culick, F. E. C., "Nonlinear Behavior of Acoustic Waves in Combustion Chambers, Parts I and II", *Acta Astronautica*, Vol. 3, 1976, pp. 714–757.

[9] Paparizos, L. and Culick, F. E. C., "The Two-Mode Approximation to Nonlinear Acoustics in Combustion Chambers. I. Exact Solutions for Second Order Acoustics", *Combustion Science and Technology*, Vol. 65, No. 5, 1989, pp. 39–65.

[10] Yang, V., Kim, S. I., and Culick, F. E. C., "Triggering of Longitudinal Pressure Oscillations in Combustion Chambers, I: Nonlinear Gasdynamics", *Combustion Science and Technology*, Vol. 72, No. 5, 1990, pp. 183–214.

[11] Yang, V., Kim, S. I., and Culick, F. E. C., "Third-Order Nonlinear Acoustic Waves and Triggering of Pressure Oscillations in Combustion Chambers, Part I: Longitudinal Modes", *AIAA 25th Aerospace Sciences Meeting*, AIAA Paper 87-1873, 1987.

[12] Culick, F. E. C., "Some Recent Results for Nonlinear Acoustics in Combustion Chambers", *AIAA Journal*, Vol. 32, No. 1, 1994, pp. 146–169.

[13] Gadiot, G. M. H. J. L. and Gany, A., "Instability Modeling with Nonlinear Pressure Coupling", *Recherche Aérospatiale*, Vol. 5, 1988, pp. 23–37.

[14] Kim, S. I., *Nonlinear Combustion Instabilities in Combustion Chambers*, PhD thesis, Pennsylvania State University, 1989.

[15] Greene, W. D., *Triggering of Longitudinal Combustion Instabilities in Rocket Motors*, Master's thesis, Pennsylvania State University, 1990.

[16] Culick, F. E. C., Burnley, V., and Swenson, G., "Pulsed Instabilities in Solid-Propellant Rockets", *Journal of Propulsion and Power*, Vol. 11, No. 4, 1995.

[17] Culick, F. E. C., "A Review of Calculations of Unsteady Burning of a Solid Propellant", *AIAA Journal*, Vol. 6, No. 12, 1968, pp. 2241–2255.

[18] Hart, R. W., Bird, J. F., and McClure, F. T., "The Influence of Erosive Burning on Acoustic Instability in Solid Propellant Rockets", Progress in Astronautics and Rocketry, Vol. 1, 1960, p. 423.

[19] McClure, F. T., Bird, J. F., and Hart, R. W., "Erosion Mechanism for Nonlinear Instability in the Axial Modes of Solid Propellant Rocket Motors", *ARS Journal*, Vol. 32, 1962, pp. 375–378.

[20] Denison, M. R. and Baum, E. A., "A Simplified Model of Unstable Burning in Solid Propellants", *ARS Journal*, Vol. 31, 1961, pp. 1112–1122.

[21] Culick, F. E. C., "Some Problems in the Unsteady Burning of Solid Propellants", Naval Weapons Center, Research Report NWC TP 4668, China Lake, CA, 1969.

[22] Ma, Y., Van Moorhem, W. K., and Shorthill, R. W., "Experimental Investigation of Velocity Coupling in Combustion Instability", *Journal of Propulsion and Power*, Vol. 7, No. 5, 1991, pp. 692–699.

[23] Jahnke, C. and Culick, F. E. C., "An Application of Dynamical Systems Theory to Nonlinear Combustion Instabilities", *Journal of Propulsion and Power*, Vol. 10, No. 4, 1994, pp. 508–517.

[24] Doedel, E., Keller, H. B., and Kernevez, J. P., "Numerical Analysis and Control of Bifurcation Problems, (I) Bifurcation in Finite Dimensions", *Intl. Journal of Bifurcation and Chaos*, Vol. 1, No. 3, 1991, pp. 493–520.

[25] Doedel, E., Keller, H. B., and Kernevez, J. P., "Numerical Analysis and Control of Bifurcation Problems, (II) Bifurcation in Infinite Dimensions", *Intl. Journal of Bifurcation and Chaos*, Vol. 1, No. 4, 1991, pp. 745–772.

Table 1. Physical Values

Propellant temperature
T_c = 300 K
Surface temperature
T_s = 880 K
Flame temperature
T_f = 3539 K
Thermal conductivity of propellant
k_p = .41868 J/m·s·K
Thermal conductivity of gas
k_g = .083736 J/m·sec·K
Thermal diffusivity of propellant
κ_p = 1.0×10^{-7} m^2/sec
Burning rate
$\bar{r}_b$ = .01145 m/sec
Activation energy
E_s/R_0 = 8011 K
Heat release on surface
Q_s = 700687 J/kg
Heat release in gas phase
Q_f = 2512080 J/kg
Average reaction rate
$\bar{w}$ = 10657.1 kg/m^3·sec
Average mass burn rate
$\bar{m}$ = 3.4 kg/m^2·sec
Specific heat of gas
c_p = 2020 J/kg·K
Specific heat of propellant
c = 1373.6 J/kg·K
Average specific heat ratio
$\bar{\gamma}$ = 1.18
Pressure exponent in burning rate law
n = .3
Temperature exponent in pyrolysis law
β_1 = 0